Molecular Therapy
Nucleic Acids
Original Article

SAP30, an oncogenic driver of progression, poor survival, and drug resistance in neuroblastoma

Philip Prathipati,[1,7] Anup S. Pathania,[2,7] Nagendra K. Chaturvedi,[3] Subash C. Gupta,[4] Siddappa N. Byrareddy,[2,5] Don W. Coulter,[3] and Kishore B. Challagundla[2,6,8]

[1]Laboratory of Bioinformatics, National Institutes of Biomedical Innovation, Health and Nutrition, 7-6-8 Saito-Asagi, Ibaraki City, Osaka 567-0085, Japan; [2]Department of Biochemistry and Molecular Biology & Fred and Pamela Buffett Cancer Center, University of Nebraska Medical Center, Omaha, NE 68198, USA; [3]Department of Pediatrics, Division of Hematology/Oncology, University of Nebraska Medical Center, Omaha, NE 68198, USA; [4]Department of Biochemistry, Institute of Science, Banaras Hindu University, Varanasi, Uttar Pradesh 221005, India; [5]Department of Pharmacology and Experimental Neuroscience, University of Nebraska Medical Center, Omaha, NE 68198, USA; [6]The Child Health Research Institute, University of Nebraska Medical Center, Omaha, NE 68198, USA

Neuroblastoma is the most devastating extracranial solid malignancy in children. Despite an intense treatment regimen, the prognosis for high-risk neuroblastoma patients remains poor, with less than 40% survival. So far, *MYCN* amplification status is considered the most prognostic factor but corresponds to only ~25% of neuroblastoma patients. Therefore, it is essential to identify a better prognosis and therapy response marker in neuroblastoma patients. We applied robust bioinformatic data mining tools, such as weighted gene co-expression network analysis, cisTarget, and single-cell regulatory network inference and clustering on two neuroblastoma patient datasets. We found Sin3A-associated protein 30 (*SAP30*), a driver transcription factor positively associated with high-risk, progression, stage 4, and poor survival in neuroblastoma patient cohorts. Tumors of high-risk neuroblastoma patients and relapse-specific patient-derived xenografts showed higher SAP30 levels. The advanced pharmacogenomic analysis and CRISPR-Cas9 screens indicated that SAP30 essentiality is associated with cisplatin resistance and further showed higher levels in cisplatin-resistant patient-derived xenograft tumor cell lines. Silencing of SAP30 induced cell death *in vitro* and led to a reduced tumor burden and size *in vivo*. Altogether, these results indicate that SAP30 is a better prognostic and cisplatin-resistance marker and thus a potential drug target in high-risk neuroblastoma.

INTRODUCTION

Neuroblastoma (neuro, nerve; blastoma, cancer) is rare cancer that develops from neuroblasts and immature nerve cells found in the adrenal glands located on top of the kidneys.[1,2] Conversely, neuroblastoma also develops in other nerve cells of the abdomen, chest, neck, spine, pelvis, and bones and can spread to other parts of the body.[2–4] Neuroblastoma is one of the topmost childhood cancers and commonly affects children under 5, rarely in older children and more commonly in boys.[5] Neuroblastoma accounts for approximately 10% of all pediatric cancer deaths.[5–7] The standard treatment for neuroblastoma includes chemotherapy, surgery, radiation, iodine 131-meta-iodobenzylguanidine (MIBG) therapy, autologous stem cell transplantation, and immunotherapy.[8–12]

The overall 5-year survival rates in children with low-risk (stages 1 to 2), intermediate-risk (stages 3 and 4S), and high-risk group (stage 4) neuroblastoma are 95%, 90%–95%, and <40%, respectively, reflecting the challenge of treating high-risk patients in the clinic. High-risk or stage 4 neuroblastoma patients frequently develop resistance to therapeutic agents due to several factors, including the communication between neuroblastoma cells and the surrounding microenvironment cells through exosomes, expression of specific oncogenes, and non-coding RNAs.[13–17] The amplification of *MYCN* (v-myc avian myelocytomatosis viral oncogene neuroblastoma-derived homolog) has been strongly associated with rapid tumor progression, worse prognosis, unfavorable histology, increased energy metabolism, and poor chemotherapy response in neuroblastoma.[6,18–20] Hence, the International Neuroblastoma Risk Group Staging System (INRGSS) identified *MYCN* amplification as a highly predictive marker of poor outcomes in neuroblastoma patients.[20–22] However, only 25% of high-risk neuroblastomas are *MYCN* amplified, indicating that the rest, 75%, are driven by factors other than *MYCN*.[23] Mass screening of neuroblastoma patients in Japan, Quebec, and Germany suggested that relapse and regression are common, even in subtypes without *MYCN* amplification.[24–26]

Dysregulation of transcriptional programs is a crucial feature of tumor progression and the acquisition of drug resistance in several human cancers.[27,28] Several genes are associated with high-risk status,

Received 27 August 2021; accepted 18 March 2022;
https://doi.org/10.1016/j.omtn.2022.03.014.

[7]These authors contributed equally

[8]Lead contact

Correspondence: Kishore B. Challagundla, Department of Biochemistry & Molecular Biology, Fred and Pamela Buffet Cancer Center, The Child Health Research Institute, University of Nebraska Medical Center, 985870 Nebraska Medical Center, Omaha, NE 68198-5870, USA.
E-mail: kishore.challagundla@unmc.edu

but not effective in disease progression, suggesting that they act as passenger genes.[29,30] Transcription factors account for about 20% of all oncogenes identified so far and are considered as "druggable" targets.[28,31–33] Chemotherapy is given to neuroblastoma patients as the first line of standard treatment. Cisplatin, the most common chemotherapy drug, is used either alone or with other chemotherapy drugs. Spontaneous tumor regression or relapse occurs in neuroblastoma at a higher frequency than in any other cancer type due to the acquisition of resistance to therapeutic agents, particularly chemotherapy drugs.[34,35] The aberrant expression of transcription factors is a feature in the progression of neuroblastoma, but the influence on drug response has not been examined so far.[36,37] Therefore, it is essential to identify a driver transcription factor that can be used as a drug response marker and further associates with stage 4, high-risk, progression, and poor survival in neuroblastoma patients.

We identified Sin3A-associated protein 30 (*SAP30*), a transcription factor meeting each of these criteria, using neuroblastoma patient datasets (The Genomics of Drug Sensitivity in Cancer and The Cancer Cell Line Encyclopedia) and CRISPR-Cas9 screens through robust bioinformatic pipelines. We also employed neuroblastoma patient tumors, patient-derived xenografts, chemo-resistant cells, and *in vivo* models in the present study. Our data demonstrate the discovery of a novel drug-response-specific driver transcription factor, which can be used as a druggable target in neuroblastoma.

RESULTS

Co-expression and motif analysis identify a distinct transcription regulator signature from three neuroblastoma patient microarray datasets

Deregulation of transcriptional program is associated with cancer progression.[27–30] So far, *MYCN* amplification is the only marker that correlates with high risk and poor prognoses in neuroblastoma. However, *MYCN* amplification addresses ∼25% of neuroblastoma, ignoring the majority of the rest, indicating an intense need to identify the transcription regulators. Thus, we aim to identify the driver transcription factors (regulators and regulons), but not the passenger genes, that can address all the risk factors, such as high risk, progression, stage 4, and death in most neuroblastoma patients. The workflow for the prioritization of neuroblastoma master regulators and the clinical characteristics of the neuroblastoma patients are given in Figure S1 and Table S1. To achieve this, we applied complementary approaches, such as co-expression and motif analysis using three neuroblastoma patient microarray datasets: GEO: GSE49710 (n = 498)[38] and GEO: GSE45547 (n = 649).[39,40] In co-expression and motif analysis,[41–44] we applied three data-mining tools to identify gene-regulatory networks: (1) weighted gene co-expression network analysis (WGCNA), which identifies biological network-based pairwise correlations between variables; (2) cisTarget, to identify DNA motifs in a gene set; and (3) single-cell regulatory network inference and clustering (SCENIC). This method incorporated three distinct steps: (1) identify sets of genes that are co-expressed with transcription factors using GENIE3, (2) perform motif analysis to establish the regulatory function of the transcription factors as regulon score, and (3) use AUCell to assess the specificity of the regulon scores across various clinical cohorts. A representative meta-analysis on the GEO: GSE49710 neuroblastoma patient dataset (n = 498)[38] is depicted in Figure 1, which shows transcription regulators differentially associated with risk status, progression, and survival in neuroblastoma patients. The specific transcription regulators that differentiate between the groups are presented according to their regulon specificity scores and highlighted in red on the plots of Figure 1.

Neuroblastoma patients in the GEO: GSE49710 (n = 498) dataset were stratified according to the risk status, progression, death, and stages. From this meta-analysis using GEO: GSE49710 (n = 498) dataset, we derived a distinct transcription regulators signature distinguishing low-risk and high-risk patients, patients with and without progression, and patients surviving versus deceased (Figure 1). The transcription regulators signature that addresses high-risk neuroblastoma status is based on E2F transcription factor 3 (*E2F3*), estrogen-related receptor alpha (*ESRRA*), Myb-like protein 2 (*MYBL2*), *SAP30*, breast cancer type 1 susceptibility protein (BRCA1), Myb-like protein 1 (*MYBL1*), nuclear transcription factor Y subunit beta (*NFYB*), Forkhead box M1 (FOXM1), transcription factor 3 (*TCF3*), and E2F transcription factor 8 (E2F8), as shown in Figure 1A. However, MYBL2 and FOXM1 were replaced by another two transcription regulators, namely E2F transcription factor 1 (*E2F1*) and E2F transcription factor 7 (*E2F7*), that address neuroblastoma progression (Figure 1B). Interestingly, we found a slightly altered transcription regulators signature in deceased patients without FOXM1 from the high-risk group and E2F7 from the progression-specific neuroblastoma patients, as depicted in Figure 1C. Our analysis in stage-specific neuroblastoma patients (Figure S2) found eight transcription regulators, namely ESRRA, E2F3, SAP30, NFYB, E2F8, MYBL1, TCF3, and BRCA1, that were similar to the high-risk group of Figure 1A transcription regulator, E2F1, which was commonly expressed in the progression-specific neuroblastoma of Figure 1B. Nonetheless, we found PHD finger protein 8 (PHF8), which was not found in any of the analysis given in Figure 1, to be a novel transcription regulator.

Furthermore, we performed a similar analysis using the GEO: GSE45547 (n = 649) dataset where patients are stratified according to the stage and MYCN amplification status (Figure S3). Stage 4 patients were shown to express a different set of regulons, such as far upstream element binding protein 1 (*FUBP1*), X-ray repair cross complementing 4 (*XRCC4*), upstream binding transcription factor (*UBTF*), TATA-box-binding-protein-associated factor 1 (*TAF1*), Tumor protein p53 (Tp53), GA-binding protein transcription factor subunit alpha (*GABPA*), and three other regulons—SAP30, E2F8, and MYBL1—that were commonly expressed in high-risk neuroblastoma patients of the GEO: GSE49710 (n = 498) dataset (Figure S3A). Besides, MYCN-amplified neuroblastoma patients showed three regulons—E2F3, SAP30, and BRCA1—that were commonly expressed in high-risk neuroblastoma patients of GEO: GSE49710 (n = 498) dataset and also distinct regulons, such as Forkhead box C1 protein (*FOXC1*), yin yang 1 (*YY1*), FUBP1, early growth response 4

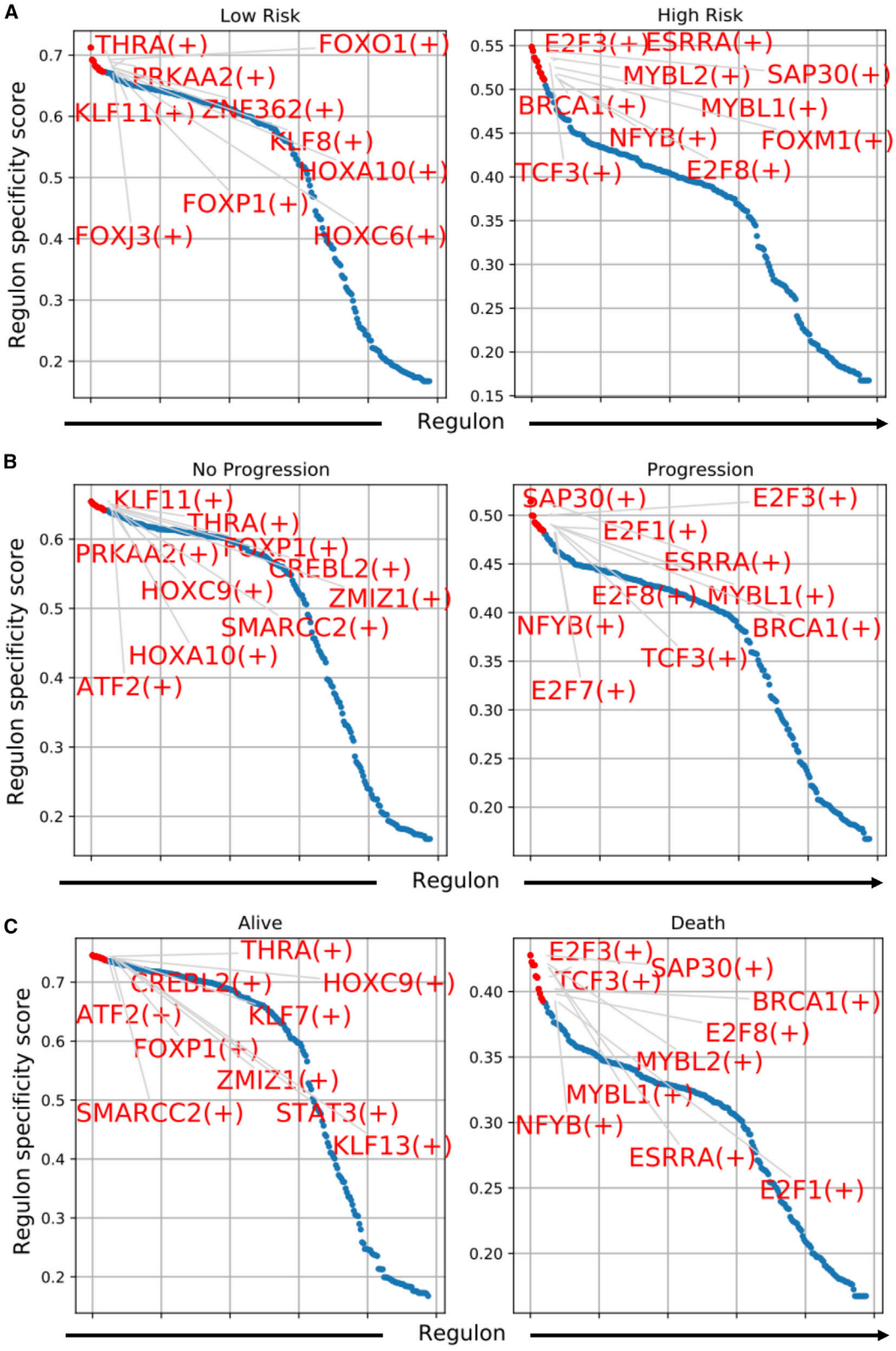

(legend on next page)

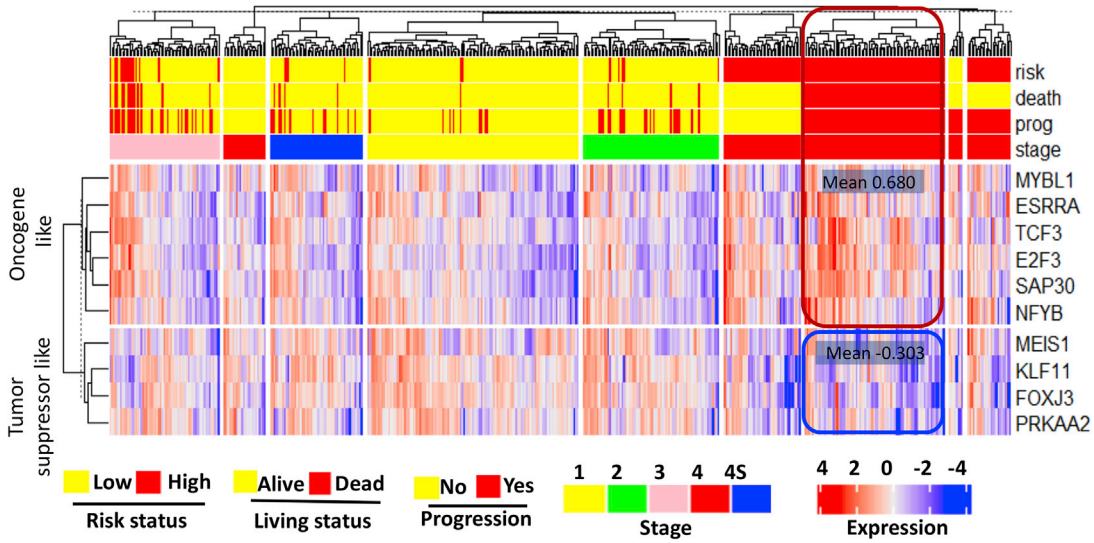

Figure 2. Differential expression analysis distinguishes the expression pattern of oncogene-like and tumor-suppressor-like transcription regulator signatures in neuroblastoma patients

The heatmap shows the stratification ability of differentially expressed transcription regulators in neuroblastoma patients (GEO: GSE49710; n = 498). Oncogene-like transcription regulators associated with high risk, death, disease progression, and stage 4 are shown in the red box (mean expression: 0.680). Tumor-suppressor-like transcription regulators are shown in the blue box of the bottom cluster (mean expression: −0.303). The labels on the right indicate transcription regulators as official gene symbols, whereas red and blue color coding represents higher and lower expression levels. Annotation tracks are given in the color key at the bottom of the heatmap, reporting neuroblastoma risk, survival, progression, and stages.

(*EGR4*), *TAF1*, T-box transcription factor 3 (*TBX3*), and B double prime 1, subunit of RNA polymerase III transcription initiation factor IIIB (BDP1), as depicted in Figure S3B. These results conclude that distinct sets of regulons are associated with stage- and *MYCN*-amplification-specific phenotypes in neuroblastoma patients.

Differential expression analysis distinguishes oncogene-like and tumor-suppressor-like transcription regulator signatures in neuroblastoma patients

The transcription regulators can act as oncogenes or tumor suppressors. Therefore, to predict the nature of these transcription regulators, we performed a stratification ability analysis per the mRNA differential expression numbers derived from the GEO: GSE49710 (n = 498) patient dataset using a hierarchical clustering approach implemented in the Bioconductor package, "complex Heatmap." A representative heatmap predicting the nature of the transcription regulators derived from this neuroblastoma patient dataset is given in Figure 2. Interestingly, our analysis identified 10 transcription regulators and classified six transcription regulators, namely MYBL1, ESRRA, TCF3, E2F3, SAP30, and NFYB, with an oncogenic signature. We also found that the other four transcription regulators—MEIS1, Kruppel-like factor 11 (KLF11), Forkhead box J3 (FOXJ3), and protein kinase AMP-activated catalytic subunit alpha 2 (PRKAA2)—appeared to have a tumor-suppressor function. The heatmap illustrates the higher expression (red box, scaled mean = 0.680) of six oncogene-like transcription factors, compared with tumor suppressors like MEIS1, KLF11, FOXJ3, and PRKAA2 (blue box, scaled mean = −0.303). The heatmap also depicts the stratification of neuroblastoma patient cohorts according to risk, survival, progression, and stage (Figure 2). Together, these results identified a higher expression of oncogene-like transcription regulators capable of stratifying neuroblastoma high-risk status, death, progression, and disease stages.

Regulon specificity score analysis indicates that SAP30 is associated with mortality, disease progression, higher risk, and stage 4 in neuroblastoma patients

Next, we analyzed the crucial transcriptional regulators and their association to the disease status. To find the relationship between each regulator and the disease status, we defined a regulon specificity score, and the modules were clustered. We used a hierarchical clustering approach implemented in the Bioconductor package, "complex Heatmap" to create a heatmap of the regulon specificity scores (Figure 3A). Our network analysis identified nine transcription regulons and

Figure 1. Identifying top transcription regulators by co-expression and motif analysis associated with the disease phenotypic status of neuroblastoma patients

Unique transcription regulators differentiate neuroblastoma patients according to the risk (A), progression (B), and survival (C) in neuroblastoma patient dataset GEO: GSE49710 (n = 498). Transcription regulators in each group are highlighted in red dots and labeled on the plot. The x axis represents different regulons, whereas the y axis indicates rank for specific transcription regulators based on the regulon specificity scores.

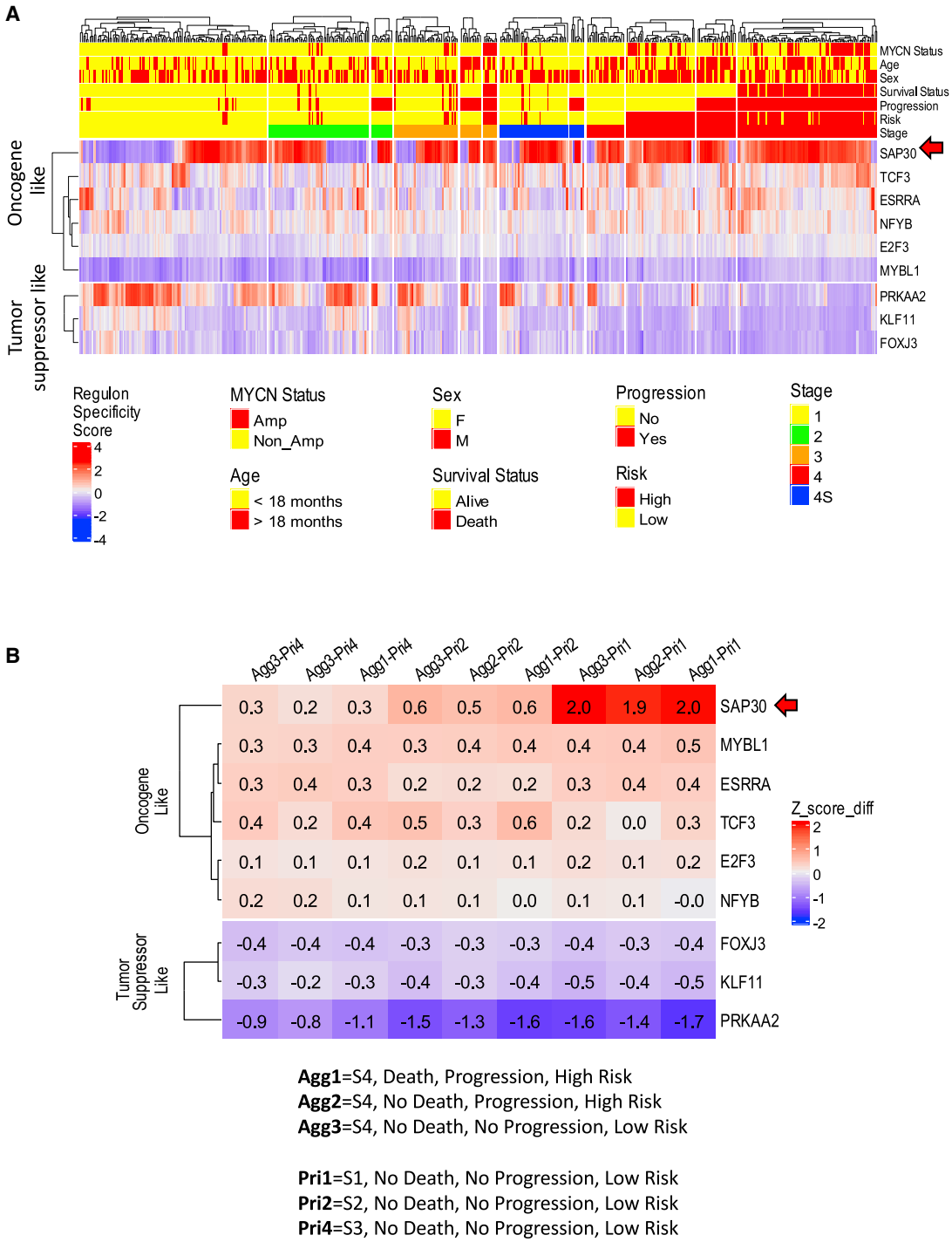

Figure 3. Regulon specificity score analysis prioritizes SAP30 for association with mortality, disease progression, high risk, and stage 4 in neuroblastoma patients

(A) The heatmap prioritizes transcription regulators based on the regulon specificity scores obtained from the neuroblastoma patient dataset GEO: GSE49710 (n = 498). The transcription regulators with high priority are given at the top, while low priority is given at the bottom. SAP30 has the highest priority score and is shown with a red arrow. The labels on the right indicate transcription regulators as official gene symbols, whereas red and blue color coding represent higher and lower regulon specificity score levels. Annotation tracks are given in the color key at the bottom of the heatmap, reporting neuroblastoma *MYCN* amplification status, age, sex, survival status, progression, risk, and stages. (B) The heatmap shows the regulon specificity score numbers and the prioritization of transcription regulators associated with different disease phenotypes

(legend continued on next page)

classified six transcription regulons, namely SAP30, TCF3, *ESRRA*, NFYB, E2F3, and MYBL1, as oncogenic signatures (Figure 3A, top cluster). We also found that other three transcription factors, such as *PRKAA2*, *KLF1*, and *FOXJ3*, appeared to have a tumor-suppressor-like function (Figure 3A, bottom cluster). The heatmap further demonstrates that the expression of SAP30 was highly specific to mortality, progression, high-risk, and stage 4 neuroblastoma patients, as shown with a red arrow in Figure 3A.

Since regulon specificity score is the key to identify specific regulons in high-risk patients, we further presented our analysis results and their score numbers in the form of a heatmap for the GEO: GSE49710 (n = 498) patient dataset. Patients were stratified as different aggregates (with or without stage 4, death, high risk, and low risk) and compared with patients of different priorities (stages S1, S2, and S3) with no death, no progression, and low risk. These results are depicted in the form of a heatmap in Figures 3B, S5A, and S5B. The data reveal that the top six regulons with major transcriptional regulatory roles in high-risk neuroblastoma are SAP30, MYBL1, *ESRRA*, TCF3, E2F3, and NFYB. The transcriptional regulators that associated with low-risk neuroblastoma are *FOXJ3*, *KLF1*, and *PRKAA2*.

To find the specificity of SAP30's highest regulon specificity score and association with mortality, progression, high risk, and stage 4 neuroblastoma patients, we performed a similar analysis using another patient dataset, GEO: GSE45547 (n = 649). The patients were stratified according to the stage and MYCN amplification status (Figure S4). However, our analysis provided a three-regulon signature, namely SAP30, MYBL1, and E2F3. In addition, we also analyzed regulon specificity score values and presented them in the form of a heatmap (Figures S5C–S5E). Patients were stratified by MYCN amplification, age and sex, and different aggregates (with or without stage 4, death, high risk, and low risk) and compared with patients of different characteristics (stages S1, S2, and S3 together with no death, no progression, and low risk). As shown in Figure S5, SAP30 was identified as the most crucial regulatory transcription factor. Together, these results conclude that SAP30 expression was a significant differentiator in all the patient group comparisons in both GEO: GSE49710 (n = 498) and GEO: GSE45547 (n = 649) patient datasets (Figures 3 and S5). Thus, we identified novel associations between SAP30 and higher risk, disease progression, and mortality in neuroblastoma patients. Then, we analyzed the distribution of the top transcriptional regulators of mRNA expression when comparing different stages of neuroblastoma patients in the GEO: GSE45547, n = 649, and EMBL: E-MTAB-179, n = 709,[45] datasets. We found that SAP30 mRNA expression distribution was significantly elevated in patients with stage 4 when compared with stage 1 (Figure 4; $p = 3.74 \times 10^{-21}$, GEO: GSE45547, n = 649; $p = 4.05 \times 10^{-7}$, EMBL: E-MTAB-179, n = 709).

High-risk neuroblastoma patients show higher SAP30 and poor survival

SAP30 is associated with high risk, disease prognosis, death, and stage 4 in neuroblastoma patient datasets (Figures 2 and 3). Next, we tested SAP30 expression in neuroblastoma patient tumor specimens. We have access to commercially available neuroblastoma patient tumor tissue microarray (US Biomax, no. NB642a), which we stained for SAP30 by immunofluorescence using SAP30-fluorescein isothiocyanate (FITC) antibody. We also have the information of risk status for the tumors. As shown in Figure 5A, higher SAP30 expression was noticed in high-risk (stage 4) neuroblastoma patients than low-risk patients (stage 1). These results confirmed that high-risk neuroblastoma patients expressed higher SAP30 and corroborated with neuroblastoma patient datasets.

We have expanded neuroblastoma-specific patient-derived xenograft tumors with the kind support of Dr. Patrick Reynolds from Texas Tech University through the Childhood Cancer Repository (https://cccells.org/), a resource laboratory of the Children's Oncology Group and the Childhood Solid Tumor Network at St. Jude Children's Research Hospital.[16] Primary tumor cells collected from neuroblastoma patients at diagnosis and progression were expanded in nude mice in our laboratory. We further explored the status of SAP30 in patient-derived xenograft tumors. We used diagnosis-specific patient-derived xenograft tumors named COG-N-424x, COG-N-496x, and COG-N-603x; progression-specific (not responding to therapy) patient-derived xenograft tumors named COG-N-453x, COG-N-470x, and COG-N-564x; and *MYCN*-amplified patient-derived xenograft tumors named SJNBL012407_x1 and SJNBL013763_x1. As shown in Figure 5B, progression-specific and *MYCN*-amplified patient-derived xenograft tumors showed a trend for higher SAP30 expression than diagnosis-specific tumors. Thus, our results confirmed the association of SAP30 in patient-derived xenograft tumors as in neuroblastoma patient datasets.

We next sought to see the SAP30 status according to the stages in other neuroblastoma patient datasets, such as GEO: GSE49710 (n = 498), GEO: GSE120572 (n = 394),[46] and PMID: 32825087 (n = 786) through R2, a web-based genomics analysis and visualization application platform. As depicted in Figure S6A, high expression of SAP30 was noticed in stage 4 patients compared with other individual stages in all three neuroblastoma patient datasets.[38,46,47] Moreover, a similar trend followed in progression, death, and non-favorable (poor prognosis) specific neuroblastoma patients GEO: GSE49710 (n = 498), compared with their respective controls (Figure S6B).[46] Since SAP30 showed higher expression in high-risk patients, we explored how SAP30 expression influences survival probability in neuroblastoma patients using GEO: GSE49710 (n = 498) and PMID: 32825087 (n = 786) datasets. Our survival analysis in neuroblastoma

obtained from the neuroblastoma patient dataset GEO: GSE49710 (n = 498). The transcription regulators with high priority are given at the top, while low priority is given at the bottom. SAP30 has the highest priority score and is shown with a red arrow. The labels on the right indicate transcription regulators as official gene symbols, whereas red and blue color coding represent a higher and lower expression of different regulons. Annotation tracks (aggregates [agg] and priority [pri]) are given at the bottom of the heatmap, reporting neuroblastoma disease phenotypes.

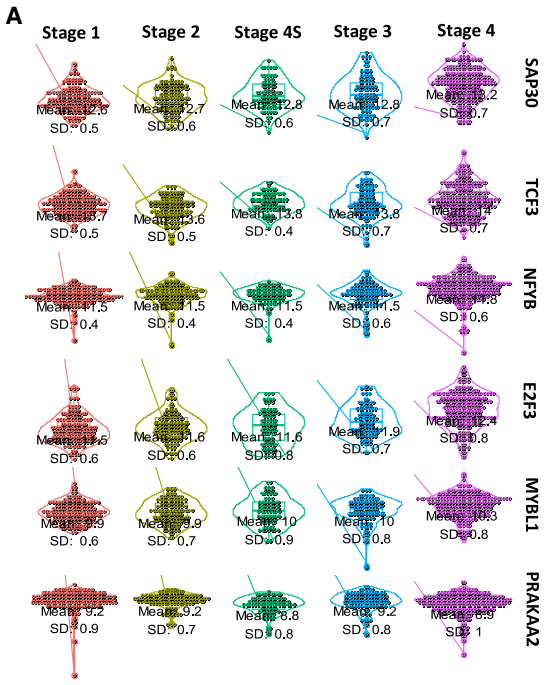

B

Regulator	P value
E2F3	1.80E-30
MYBL1	2.18E-09
NFYB	2.47E-16
PRKAA2	2.78E-06
SAP30	3.74E-21
TCF3	5.03E-06

D

Regulator	P value
E2F3	2.37E-19
ESRRA	2.68E-03
FOXJ3	9.37E-15
KLF11	1.72E-12
MYBL1	9.73E-02
NFYB	3.32E-02
PRKAA2	8.21E-13
SAP30	4.05E-07
TCF3	9.85E-03

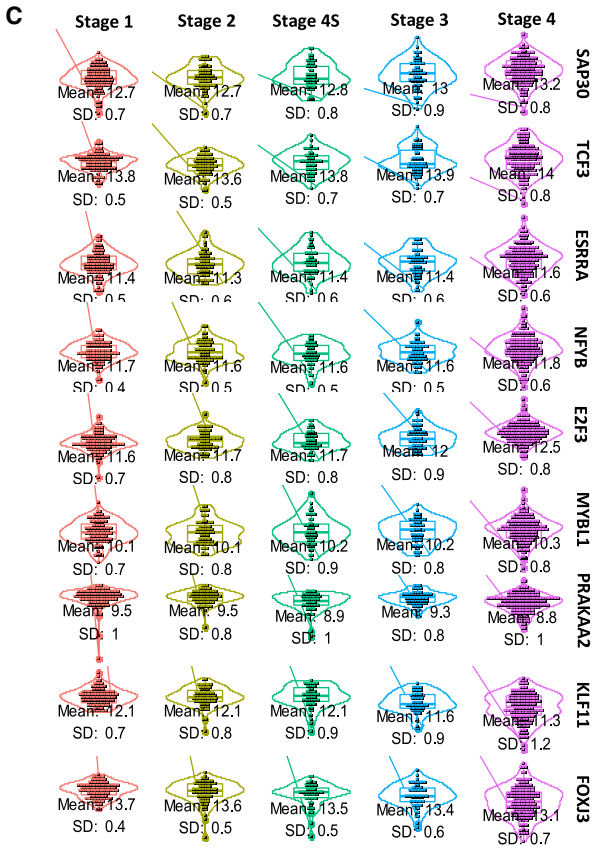

Figure 4. The distribution pattern of transcription regulators in neuroblastoma patients

Violin plots show the distribution of transcription regulators expression in different stages of neuroblastoma, in patient datasets GEO: GSE45547, n = 649 (A), and EMBL: E-MTAB-179, n = 709 (C). The significance of the differences between different stage patients was determined by an unpaired t test (B and D).

patients in the R2 database revealed a remarkable statistically significant correlation between higher SAP30 expression and poor survival in neuroblastoma patients (Figures 5C and 5D).[38,46–49] These results collectively concluded that high-risk neuroblastoma patients expressed higher SAP30, which was associated with poor survival.

Advanced pharmacogenomic analysis and CRISPR-Cas9 screens indicate that SAP30 activity correlates with cisplatin resistance in neuroblastoma cell lines

SAP30's DNA-binding domain 3D coordinates extracted from a nuclear magnetic resonance (NMR)-derived structure (PDB: 2LD7)[50] are shown in Figures 6A and 6B. For neuroblastoma patients, including high risk, cisplatin is a functional chemotherapy agent.[51] However, neuroblastoma cells can exhibit innate and acquired resistance to cisplatin.[52] Thus, studies finding an effective marker that predicts therapy response, higher risk, disease progression, stage, and mortality in neuroblastoma patients are lacking. Since SAP30 is strongly associated with higher risk, disease progression, stage, and mortality in neuroblastoma patients and patient datasets, we investigated how chemotherapy resistance would relate to SAP30 expression.

We performed a comprehensive bioinformatic analysis integrating heterogeneous molecular data from the Genomics of Drug Sensitivity in Cancer (GDSC)[53] and the Cancer Cell Line Encyclopedia (CCLE)55 databases. These databases contain three types of information: (1) response to cisplatin in the form of half-maximal inhibitory concentration (IC_{50}); (2) response to various bromodomain-containing protein 4 (BRD4) inhibitor drugs (AZD5153, I-BET-762, JQ1, OTX015, PFI-1, and RVX-208) in ~1,000 human cancer cell lines, including neuroblastoma;[53,54] and (3) genome-wide CRISPR-Cas9 fitness or gene essentiality screens in response to single-guide RNA (sgRNA)-based knockout of ~18,500 genes, which enable the prioritization of genes essential for

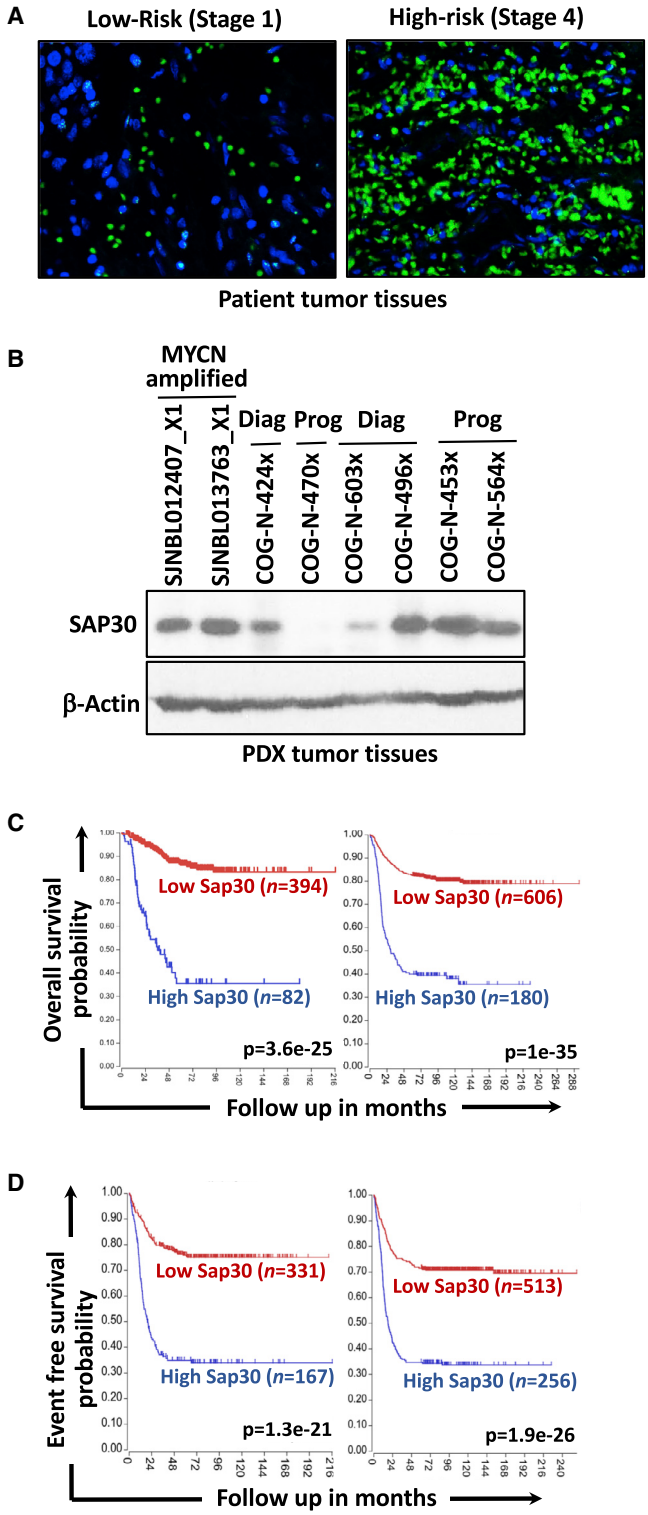

Figure 5. SAP30 associates with high-risk status and poor survival in neuroblastoma patients

(A and B) Immunofluorescence (A) and western blotting (B) image of SAP30 in low- and high-risk neuroblastoma patients (A), and *MYCN*-amplified, diagnosis- and progression-specific patient-derived xenograft (PDX) tumors (B). (C and D) Kaplan-Meier curves show the correlation between expression of SAP30 and overall survival (C) or event-free survival (D) from two independent patient datasets GEO: GSE49710, n = 498 (left), and PMID: 32825087, n = 786 (right). Patients with higher SAP30 had a shorter survival.

cell viability or growth.[55–60] We merged neuroblastoma cell line data from these two databases and performed a robust correlation analysis. As shown in Figure 6C, SAP30 essentiality showed a significant negative correlation with cisplatin IC_{50} values (R = −0.73; p = 0.061). Neuroblastoma growth critically depends on epigenetic factors, in particular BRD4. Therefore, to see the specificity of SAP30 on cisplatin therapy response, we further verified the essential role of SAP30 on BRD4-inhibitor response. As depicted in Figure 6D, we observed a positive correlation (R = 0.75; p = 0.031) with a potent BRD4 inhibitor (AZD5153) LN IC_{50} values, demonstrating that SAP30 essentiality is associated with cisplatin resistance but sensitive to other drugs like BRD4 inhibitors. These results indicate SAP30 is a specific cisplatin resistance marker in neuroblastoma.

To validate these findings, we further tested the expression of SAP30 in two cisplatin-resistant patient-derived xenograft tumor cell lines that we developed in our laboratory. The resulting two resistant cell lines (COG-N-424 and COG-N-496) had initial and final IC_{50} concentrations of 1.2 μM, 7.4 μM, 3 μM, and 16 μM, respectively, and were used for our preliminary experiments. As shown in Figure 6E, both of these cell lines showed higher SAP30 than their respective parental control cells. Altogether, these results indicate that SAP30 is a cisplatin-therapy-resistant marker in neuroblastoma.

Silencing of SAP30 induces cell death in neuroblastoma cells

To investigate the effect of SAP30 in the progression of neuroblastoma, we generated SAP30 knockdown stable SK-N-BE(2)c, SK-N-AS, and NB19 neuroblastoma cell lines and studied various functional assays. The knockdown efficiencies of two individual short hairpin RNAs (shRNAs) against SAP30 were tested in three neuroblastoma cell lines (Figure 7A). Using a cell viability assay, we observed significant reduction of neuroblastoma cell growth upon knockdown of SAP30, compared with control shRNA cells (Figure 7B). Further, to see the effect of SAP30 on cell death, we performed dead cell analysis using 7-aminoactinomycin D (7-AAD) staining by flow cytometry. The representative dot plots of 7-AAD staining and the percentages of dead cells are shown in Figure 7C. As shown, silencing of SAP30 using two shRNAs targeting at two different loci in the SAP30 mRNA coding sequence significantly increased the percentage of dead cells in SK-N-AS (6.9%–12.7%) and NB19 (11.2%–19.2%) cells. Taken together, these results indicate that SAP30 silencing induces apoptosis in SK-N-AS and NB19 cells, suggesting oncogenic potential for SAP30.

Silencing of SAP30 induces a reduction in mitochondrial membrane potential in neuroblastoma cells

Mitochondrial membrane potential is a valued indicator of health status in cells, and changes in the mitochondrial membrane permeability are considered as an early event in the process of apoptosis. The

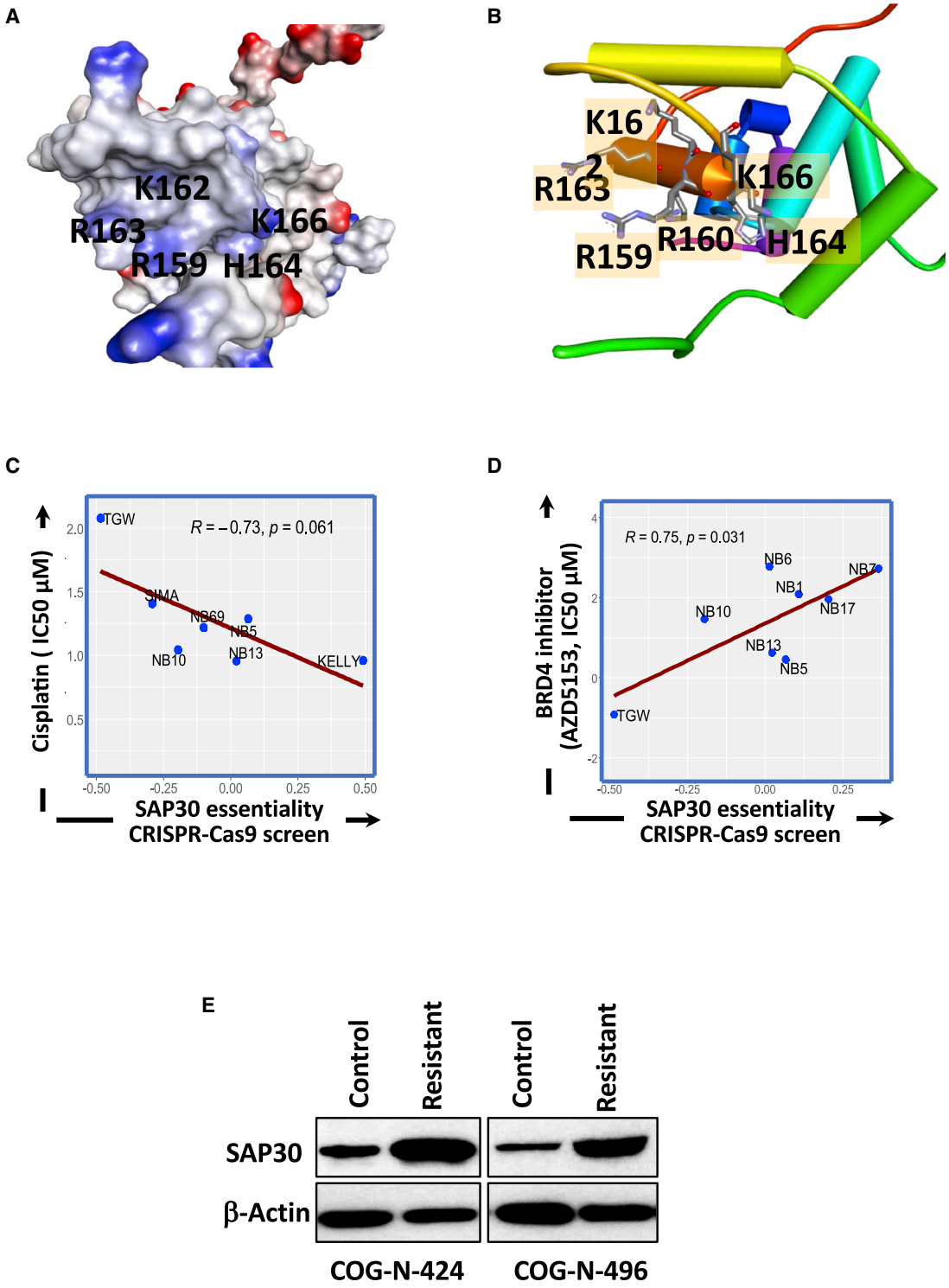

Figure 6. Cisplatin resistant patient-derived xenograft tumors cells express higher SAP30

(A and B) Molecular surface (A) and schematic representation (B) of SAP30's DNA domain, with residues (R, arginine; K, lysine; H, histidine) comprising the nucleolar localization sequence that mediate DNA binding highlighted. (C and D) CRISPR-Cas9 essentiality screen data of neuroblastoma cells show resistance to cisplatin (C) but sensitivity to BRD4 inhibitor drugs (D). (E) Western blotting image of SAP30 in two cisplatin-resistant neuroblastoma cells derived from patient-derived xenograft tumors.

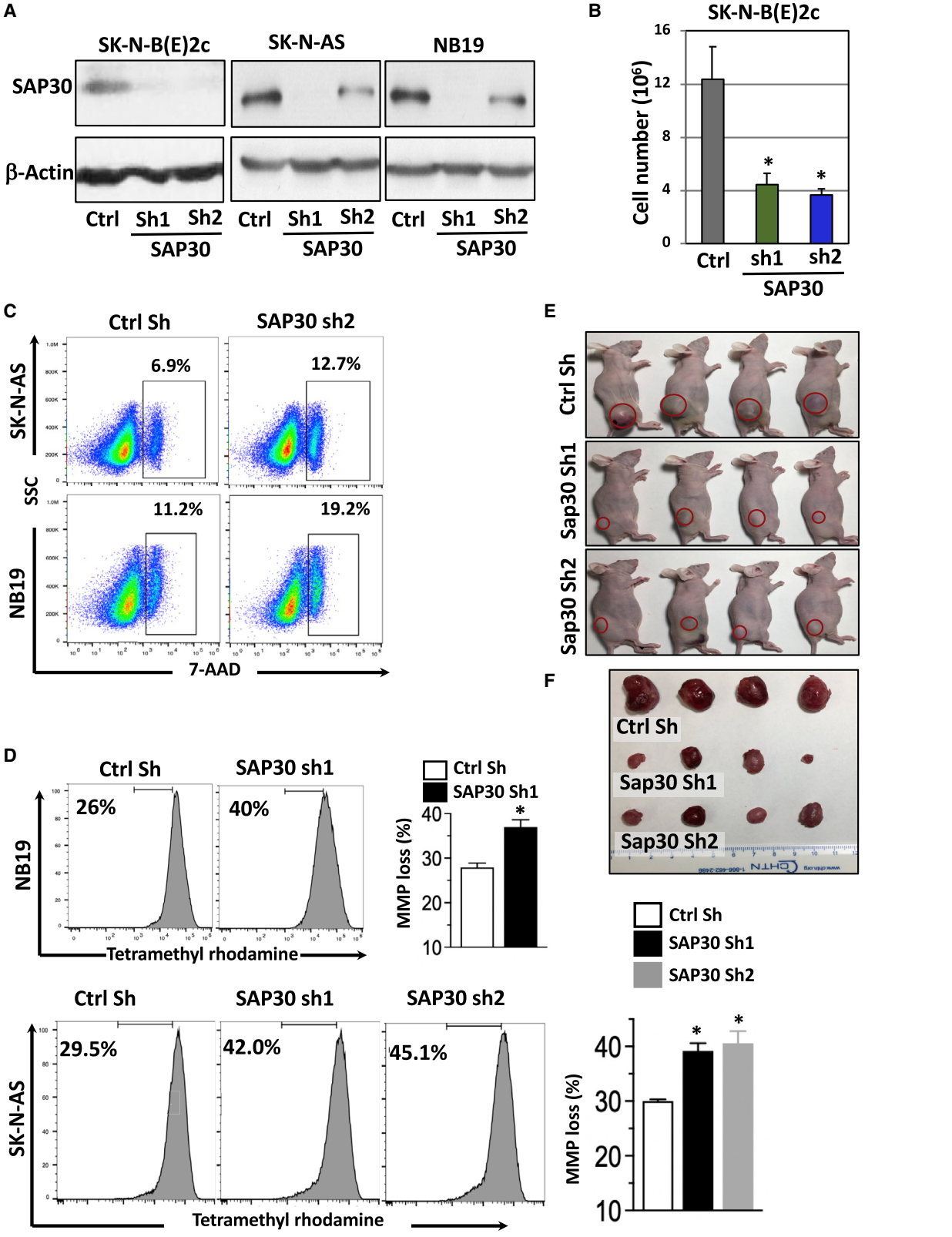

(legend on next page)

enzymes involved in the mitochondrial electron transport chain influence the generation of mitochondrial membrane potential. The collapse of mitochondrial membrane potential coincides with the opening of the pores responsible for the mitochondrial permeability transition that triggers the downstream events of the apoptotic signaling cascade. We used flow cytometry to elucidate possible mitochondrial involvement in SAP30-regulated cell viability. Tetramethylrhodamine, a sensitive fluorescent probe, was used as an indicator of mitochondrial dysfunction in SK-N-AS and NB-19 cells. As depicted in Figure 7D, the tetramethylrhodamine assay showed that silencing SAP30 in neuroblastoma cells induced a drop in mitochondrial membrane potential. These results suggest that silencing of SAP30 induces cell death in SK-N-AS and NB-19 cells through altering mitochondrial function in neuroblastoma cells. Taken together, these results indicate that SAP30 acts as an oncogene in neuroblastoma cells *in vitro*.

Silencing of SAP30 reduces tumor growth in neuroblastoma xenografts *in vivo*

Our *in vitro* data have shown that SAP30 acted as an oncogene. To confirm the tumor-promoting role of SAP30 *in vivo*, we established a subcutaneous tumor xenograft model using non-obese diabetic (NOD) severe combined immunodeficiency (SCID) gamma (NSG) mice. All the animal experiments were performed under a protocol approved by the Institutional Animal Care and Usage Committee (IACUC) of University of Nebraska Medical Center (UNMC). First, we established SAP30 knockdown SK-N-B(E)2c stable cells (Figure 7A). Cells were subcutaneously implanted (4×10^6/100 μL PBS/Matrigel) for 35 days using our previously established xenograft model.[13] As depicted in Figures 7E and 7F, the tumor burden and size were reduced in mice receiving a subcutaneous injection of cells in which Sap30 was knocked down by shRNA. Overall, our data indicate that the changes in the tumor formation are due to the oncogenic effect of Sap30, which can thus be considered as an oncogene in neuroblastoma.

DISCUSSION

Neuroblastoma patients are a particularly high-risk group that pose complex challenges for clinical treatment. Although significant progress has been made, and most patients achieve remission post-chemotherapy treatment, relapse is considered a significant problem in treating patients. This is due to the acquisition of a resistance phenotype by cancer cells. So far, MYCN status is considered the most critical prognostic factor in neuroblastoma patients. MYCN transcription factor belongs to the family of MYC oncoproteins that include c-Myc, L-Myc, and N-Myc.[61] The expression of MYCN is limited to hematopoietic stem cells and cells within the developing nervous system.[16,62–65] The aberrant expression of MYCN has been shown in tumors of neural cell origins, such as neuroblastoma, glioblastoma, medulloblastoma, retinoblastoma, and astrocytoma.[21,61,66] Recent experiments in neuroblastoma patients, cell lines, and zebrafish models suggested that progression of non-*MYCN*-amplified neuroblastoma is predominantly driven by c-MYC and that c-MYC and *MYCN* expression seems mutually exclusive.[67–69] However, *MYCN* addresses only 25% of neuroblastomas, and thus, it is urgent to identify markers that predict chemotherapy response among high-risk patients, including those with higher progression and an outcome of mortality.

Three clinical trials, NB90, NB97, and NB2004, were conducted in 66 community hospitals in Germany and Switzerland through the German Pediatric Oncology Society to analyze a subpopulation of patients diagnosed before 18 months of age and classified within in the high-risk MYCN non-amplified population. All these patients were treated with a variety of chemotherapy drugs. These studies revealed that stage 4 patients aged less than 18 months of age showed a more favorable prognosis than the older patients but were prone to secondary malignancies, such as ganglioneuroma.[70] Thus, identified age (<18 months) indicates a favorable prognosis in stage 4 patients. Researchers and clinicians across the globe have put enormous efforts into increasing survival in neuroblastoma patients. A study through the International Neuroblastoma Risk Group database (1974–2002) involving 11,307 patients across Australia, Europe, Japan, and North America provided evidence of a consistent enhancement of overall survival during stages 1, 2, 3, and 4S but unchanged survival in stage 4 patients.[71] An Italian Neuroblastoma Registry study involving 2,216 children diagnosed between 1979 and 1984, 1985–1991, 1992–1998, and 1999–2005 (age 0–14 years) was analyzed to determine the relative risk of second malignant neoplasm and overall survival.[72] Results indicated a progressive improvement of overall survival in stages 1 and 3 and further showed a significant risk of second malignant neoplasm in long-term survivors but a slight improvement in patients with stage 4 disease between the first- and second-time cohorts, but not later.[72] However, no specific information was available on stage 4 patients. Taken together, these studies addressed survival patterns in patients belonging to the low- and intermediate-risk groups.

A study led by Capasso et al. derived a risk-scoring system according to a set of 18 gene expressions that can predict the overall survival of stage 4 neuroblastoma patients (n = 342).[73] Immunotherapy by

Figure 7. SAP30 knockdown inhibits cell viability, induces cell death and mitochondrial membrane potential in neuroblastoma cells *in vitro*, and reduces tumor burden *in vivo* in a mouse xenograft model of neuroblastoma

(A–D) A representative (A) western blotting image of SAP30 showing the knockdown efficiency, (B) quantification graph of cell viability assay evaluating the effect of SAP30 silencing on cell proliferation, and (C and D) flow cytometry pictures and quantification graphs of (C) cell death analysis and (D) mitochondrial membrane potential in neuroblastoma cells upon stable knockdown of SAP30 using two different shRNAs. (E and F) Tumor burden in (E) NOD/SCID mice receiving a subcutaneous injection of SK-N-B(E)2c cells with SAP30 stably silenced using two different shRNAs and (F) images of the excised tumors of the mice from various treatment groups are given. The data presented are the mean ± SD of three independent experiments. p values were calculated using two-tailed unpaired t tests between SAP30 knockdown and control cells. *$p < 0.05$.

treatment with Unituxin, a chimeric GD2 antibody, has been promising for high-risk neuroblastoma patients. Although high-risk neuroblastoma is heterogeneous, similar immunotherapy treatment is being given without additional risk stratification, and limited studies have focused on this stratification.[46,74] Thus, it is crucial to stratify the high-risk neuroblastoma patients into subgroups for personalized treatment. A group led by Wang derived an immune-related gene expression signature that distinguishes the subtypes of high-risk neuroblastoma patients. Kinases with oncogenic and tumorigenic properties in several human cancers have been well characterized in terms of overexpression or dysregulation.[75–77] Therefore, attempts have been made to profile kinome expression by an unbiased approach in high-risk neuroblastoma tumors. This work elucidated a kinome signature of 27 proteins called Kinome-27 that distinguish responders and non-responders to suberoylanilide hydroxamic acid (SAHA) and radicicol.[78] High-risk neuroblastoma is associated with the development of resistance to chemotherapy drugs like cisplatin, and relapsed patients have a poor prognosis, resulting in a severe clinical problem. Studies have been done to identify a vincristine resistance gene signature in resistant neuroblastoma cells, aimed at predicting the prognosis of high-risk neuroblastoma patients.[79] In addition, proteomic signatures were analyzed in cisplatin-resistant UKF-NB-4 neuroblastoma cells by nano-liquid chromatography with tandem mass spectrometry. This experiment identified several families of proteins involved in proteasome activity and enriched in the lysosomes of cisplatin-resistant cells, offering evidence that these pathways are responsible for intrinsic chemo-resistance to cisplatin.

However, all these studies were focused on patients stratified according to their group, age, MYCN amplification, or chemotherapy drugs, but not patients stratified by disease progression, death, stage 4, high risk, and termed as ultra-high-risk neuroblastoma patients. By applying novel, robust bioinformatic methodologies, such as WGCNA to identify network-based pairwise correlations between different disease variables, cisTarget to identify DNA motifs in a set of genes, and SCENIC analyses to identify gene-regulatory networks,[41–44] we identified a unique transcription regulator signature that distinguishes high risk from low risk, higher progression from lower, stage 4 from the other stages, and dead from live patients. We applied these analyses to a group totaling 1,252 patients that belong to three patient datasets. The clinical characteristics of the patients from these three datasets are different. For example, survival status, progression, risk, and stages are available in the dataset GEO: GSE49710 (n = 498); stage and *MYCN* amplification are available in the dataset GEO: GSE45547 (n = 649); and MYCN amplification, risk, the status of 11q (deletion, normal, and whole loss), the status of 17q (gain, normal, and whole gain), the status of 1p (deletion, gain, and normal), and stage are available in the dataset GEO: GSE73517 (n = 105). Hence, we believe this explains the variation in the number of transcription factors identified in each dataset. We shortlisted SAP30 from the unique transcription regulator signature based on its regulon score and its identification in all three datasets. Thus, we prioritized SAP30 further in our studies and ensured the novelty of the studies. Importantly, identifying the novel driver transcription factor, SAP30, as a drug resistance oncogenic marker can help identify non-chemotherapy-responsive patients, and this gene is a promising drug target in high-risk neuroblastoma patients.

CONCLUSIONS

(1) For the first time, a unique transcription regulator signature is derived from high-risk neuroblastoma patients through a combination of machine-learning approaches, such as WGCNA, cisTarget, and SCENIC, in patient cohorts. This signature is further validated in two other patient cohorts. (2) Based on the regulon specificity score, we prioritized SAP30, a driver transcription factor positively associated with high-risk, higher progression, stage 4, and poor survival in neuroblastoma patients. (3) Tumors of high-risk neuroblastoma patients and relapse-specific patient-derived xenografts showed higher SAP30 levels. (4) Genomics of Drug Sensitivity in Cancer, the Cancer Cell Line Encyclopedia databases, and CRISPR-Cas9-based SAP30 essentiality showed resistance to cisplatin, but not for other epigenetic drugs. (5) Cisplatin-resistant patient-derived xenograft tumor cell lines showed higher SAP30 levels, and further silencing of SAP30 in cells induced cell proliferation. (6) Silencing of SAP30 reduced cell proliferation, cell death *in vitro*, and tumorigenicity *in vivo*. (7) Thus, SAP30 is considered a better prognostic and chemotherapy-resistant marker than *MYCN* and could be considered a potential drug target for high-risk neuroblastoma patients. However, the mechanistic insight behind SAP30-mediated oncogenicity and drug resistance is another area of investigation.

MATERIALS AND METHODS

Neuroblastoma patient datasets, data mining, and survival analysis

Data from a total of 1,252 patients of three datasets named as GEO: GSE49710 (n = 498) and GEO: GSE45547 (n = 649) were downloaded from NCBI Gene Expression Omnibus (https://www.ncbi.nlm.nih.gov/geo/). Neuroblastoma patients from the GEO: GSE49710 cohort were predominantly Chinese, whereas GEO: GSE45547 and GEO: GSE73517 cohorts were predominantly German. Additional datasets EMBL: E-MTAB-179 (n = 709), GEO: GSE120572 (n = 394), and PMID: 32825087 were also used for analyzing survival graphs. Disease stages and risk status were categorized according to the International Neuroblastoma Staging System (INSS)[80] and the International Neuroblastoma Risk Group (INRG) classification system.[81] The detailed clinical characteristics of neuroblastoma patients, such as sex, *MYCN* amplification, risk status, and progression are presented in Table S1. All the raw data and normalized data were available through the GEO databases. Patients' RNA sequencing (RNA-seq) and microarray-based gene-expression matrices and clinical information were directly downloaded for the analyses. All the data were processed through R software (https://www.r-project.org/). R2, a web-based genomics analysis and visualization application platform (http://r2.amc.nl) developed by the Academic Medical Center in Amsterdam (the Netherlands) was used to investigate the expression of Sap30 and its relationship with overall survival probability. We obtained microarray analysis results from publicly available neuroblastoma patient cohort data.[49] Characteristics of the patients were

published earlier.[49] We used a hierarchical clustering approach implemented in the Bioconductor package, complex Heatmap for Figure 3.

Patient tumor tissues and immunofluorescence staining

De-identified formalin-fixed and embedded paraffin blocks of neuroblastoma patient tissue microarray (no. NB642a) were obtained from US Biomax (26 patients' samples, in duplicates). Our institutional ethics committee approved the use of the neuroblastoma patient tissue microarray. Immunofluorescence staining for SAP30 protein was performed through our institutional core facility on a Discovery Ultra staining system (Roche Tissue Diagnostics, Ventana Medical Systems), as previously described. In brief, tissue sections were deparaffinized using a mild detergent solution at 69°C for 24 min followed by antigen retrieval at 95°C for 32 min. Sections were further treated with Discovery Chromo Map inhibitor at 37°C for 8 min. Immunofluorescent staining was performed using mouse monoclonal SAP30 (131–219) primary antibody (Novus Biologicals, 1:400 dilution, Catalogue H00008819-M02) and Discovery FITC kit (RUO) for 12 min and counterstained with DAPI for DNA staining for 8 min (Roche Diagnostics). Immunofluorescence images were analyzed, imaged, and photographed using a Zeiss LSM 710 confocal microscope.

Patient-derived xenografts

Neuroblastoma-specific patient-derived xenograft tumors, namely COG-N-415x, COG-N-440x, COG-N-561x, COG-N-660x, COG-N-620x, COG-N-426x, SJNBL012407_x1, and SJNBL013763_x1, were established in collaboration with Dr. C. Patrick Reynolds and the Childhood Solid Tumor Network at St. Jude Children's Research Hospital.[16] Patient tumor tissues were surgically removed and cut into multiple pieces in sterile Hank's balanced salt solution (HBSS) supplemented with antibiotics in Dr. Reynolds's laboratory. De-identified tumor tissues were received through the Children's Oncology Group Cell Culture and Xenograft Repository (http://www.cogcell.org). Tumor tissues were subcutaneously injected into 4- to 6-week-old nude mice. After xenograft transplantation, animals were observed for palpable tumors. When tumors reached ~1,500 mm^3, the animals were euthanized and tumors were excised and used for the western blotting analysis. The average time for tumor growth was noted to be 60 days (ranging from 30 to 120 days). The UNMC institutional ethics committee approved the study methodologies.

Cell lines and culture conditions

SK-N-BE(2)c, NB19, and SK-N-AS human neuroblastoma cells were obtained from American Type Culture Collection (ATCC). COG-N-424 and COG-N-496 cell lines were developed in our laboratory from their respective patient-derived xenograft tumors with the kind support of Dr. C. Patrick Reynolds through the Children's Oncology Group Cell Culture and Xenograft Repository (http://www.cogcell.org). These cells were used to develop cisplatin-resistant cell lines by culturing them in increasing concentrations of cisplatin over 7 months, as described previously.[17] The resulting two resistant cell lines (COG-N-424 and COG-N-496) had initial and final IC_{50} concentrations of [1.2 μM, 7.4 μM] and [3 μM, 16 μM], respectively. Cell lines were cultured at 37°C in a 5% CO_2 humidified atmosphere in Roswell Park Memorial Institute (RPMI) media containing 10% heat-inactivated fetal bovine serum (FBS) supplemented with penicillin and streptomycin (50 U/mL), L-glutamine, sodium pyruvate, and non-essential amino acids as described earlier. Before use, all cell lines were authenticated by DNA profiling and were frequently tested to confirm they were free from mycoplasma.[13]

Western blotting and antibodies

Western blotting analysis was performed as described previously.[13,82] In brief, cells from the experiments were lysed in radioimmunoprecipitation assay (RIPA) lysis buffer with protease and phosphatase inhibitors and incubated on ice for 15 min, followed by sonication. The resulting lysates were centrifuged at 15,000 rpm for 15 min to get cleared supernatants, and protein concentration was determined using the Bradford protein assay reagent. Cleared lysates were resolved by SDS gel electrophoresis using the mini-PROTEAN Tetra System (Bio-Rad), and proteins were transferred to polyvinylidene difluoride membranes. The membranes were incubated with either rabbit monoclonal anti-Sap30 (Novus Biologicals; 1:1,000 dilution; cat no. NBP1-92648) or horseradish peroxidase (HRP)-conjugated anti-β-actin (Proteintech; 1:12,000; cat no. HRP60008) overnight at 4°C, followed by incubation with secondary antibodies 1 h at room temperature, and then developed using an enhanced chemiluminescence reagent system.

Advanced pharmacogenomic analysis and CRISPR-Cas9 screens

The Welcome Trust at the Sanger Institute (UK) and the Center for Molecular Therapeutics at the Massachusetts General Hospital Cancer Center (USA) conducted The Genomics of Drug Sensitivity in Cancer (GDSC) Project (http://www.cancerrxgene.org/) to identify cancer biomarkers that can be used to identify patients most likely to respond to cancer therapies.[83] This project screened more than 1,000 genetically characterized human cancer cell lines and a wide range of anti-cancer therapeutics, including cytotoxic chemotherapeutic drugs. The cell lines' sensitivity patterns were correlated with genomic and expression data to identify genetic features that can predict sensitivity to these drugs. The Broad Institute and the Novartis Institutes for Biomedical Research started CCLE project to characterize a large panel of human cancer models and link with distinct pharmacologic vulnerabilities and genomic patterns, including CRISPR-Cas9 screen data to translate cell line integrative genomics into cancer patient stratification.[54] We used these datasets for the analysis of cells' responses to various chemo drugs in the presence of specific gene knockouts.

Short hairpin RNAs, lentiviral vectors, and the establishment of stable knockdown cell lines

We generated shRNA-mediated SAP30 stable knockdown cells using a lentiviral expression system through an established method.[13] Lentiviral plasmids expressing SAP30-specific shRNAs (SHCLNG-NM_002931, TRCN0000021989, and TRCN0000021990) and non-targeting control shRNAs (SHC002V) were purchased in bacterial

glycerol stock (MISSION Lentiviral shRNAs, Sigma, MO). Plasmids were amplified and isolated from the bacterial stocks using the PureLink HiPure Plasmid Maxiprep Kit (Thermo Fisher Scientific, Waltham, MA). Briefly, lentiviral particles were generated in HEK293T cells (3×10^6; 10 cm dish) growing in 10% fetal calf serum (FCS)-DMEM medium (8 mL) by transfecting with lentiviral shRNA construct (10 μg) and lentiviral packaging plasmids containing pVSV-G (5 μg), pMDL (10 μg), and pREV (5 μg) using polyethylenimine (PEI) transfection reagent (DNA: PEI, 1:4 ratio) for 24 h followed by replacing media with fresh 10% FCS-DMEM. After 48 and 72 h, the medium was collected and centrifuged at 1,000 rpm for 5 min at 20°C followed by filtration using a 0.45-μm syringe filter. According to the manufacturer's instructions, the lentiviral particles were concentrated using PEG-it Lentivirus Concentration solution (LV810A-1/LV825A-1, System Biosciences, Palo Alto, CA) and used for infection of neuroblastoma cells SK-N-BE(2)c, SK-N-AS, and NB-19. Neuroblastoma cells (10^5 cells/well) were seeded in a 6-well plate and infected with lentivirus particles when approaching 40% confluence at 37°C for 24 h. Following viral infection, the shRNA viral particle-containing medium was replaced with a fresh medium containing puromycin (2–5 μg/mL) for 3–5 days to select transduced cells. The selection medium was changed every 2 days. The cells were tested for the knockdown efficiency of Sap30 by western blotting analysis and used for the experiments.

Statistical analysis

The data were expressed as mean ± standard deviation. The difference between two treatment groups was analyzed using Student's t test. One-way analysis of variance (ANOVA) was used for the comparisons between more than two groups. The data analysis was carried out using GraphPad Prism 7.0 software. A value of $p < 0.05$ was considered statistically significant. Kaplan-Meier curves and gene correlation plots were prepared using the R2: Genomics Analysis and Visualization Platform (http://r2.amc.nl). Multiple expression quantiles were explored, and the optimal cutoff is defined as the expression quantile with the most significant (log rank test) split. Hazard ratios (HRs), including 95% confidence intervals, were calculated.

SUPPLEMENTAL INFORMATION

Supplemental information can be found online at https://doi.org/10.1016/j.omtn.2022.03.014.

ACKNOWLEDGMENTS

Dr. Challagundla's laboratory is supported by NIH/NCI grant CA197074; the State of Nebraska and the Pediatric Cancer Research Group, part of the Child Health Research Institute; and Department of Biochemistry & Molecular Biology start-up funds. We are grateful to Jonas Nance and Kristyn McCoy at the Childhood Cancer Repository (supported by Alex's Lemonade Stand Foundation) and Dr. Åsa Karlström at the Childhood Solid Tumor Network of St. Jude Children's Research Hospital for arranging neuroblastoma patient-derived xenograft tumor cells, Sita Devi for data mining from the R2 database, and the Tissue Sciences Facility of UNMC for immunofluorescence staining. The authors would like to thank Matthew Sandbulte, Child Health Research Institute at Children's Hospital & Medical Center, and UNMC for editorial assistance.

AUTHOR CONTRIBUTIONS

P.P., A.S.P., and K.B.C. designed studies; performed patient data mining, survival, and correlation analyses; expanded patient-derived xenografts; performed experiments; analyzed data; and wrote the first draft of the manuscript. N.K.C. provided neuroblastoma cell lines, S.N.B. assisted in flow cytometry experiments, and S.C.G. and D.W.C. provided suggestions to the study design and assisted in manuscript preparation, review, and edits. K.B.C. acquired funding, coordinated with all coauthors, and supervised the project.

DECLARATION OF INTERESTS

The authors declare no competing interests.

REFERENCES

1. Mahapatra, S., and Challagundla, K.B. (2020). Cancer, Neuroblastoma. (StatPearls).
2. Cushing, H., and Wolbach, S.B. (1927). The transformation of a malignant paravertebral sympathicoblastoma into a benign ganglioneuroma. Am. J. Pathol. *3*, 203–207.
3. Johnsen, J.I., Dyberg, C., and Wickström, M. (2019). Neuroblastoma-A neural crest derived embryonal malignancy. Front. Mol. Neurosci. *12*, 9.
4. Nakagawara, A., Li, Y., Izumi, H., Muramori, K., Inada, H., and Nishi, M. (2018). Neuroblastoma. J. Clin. Oncol. *48*, 214–241.
5. Brodeur, G.M. (2003). Neuroblastoma: biological insights into a clinical enigma. Nat. Rev. Cancer *3*, 203–216.
6. Seeger, R.C., Brodeur, G.M., Sather, H., Dalton, A., Siegel, S.E., Wong, K.Y., and Hammond, D. (1985). Association of multiple copies of the N-myc oncogene with rapid progression of neuroblastomas. N. Engl. J. Med. *313*, 1111–1116.
7. Irwin, M.S., and Park, J.R. (2015). Neuroblastoma: paradigm for precision medicine. Pediatr. Clin. North Am. *62*, 225–256.
8. Colon, N.C., and Chung, D.H. (2011). Neuroblastoma. Adv. Pediatr. *58*, 297–311.
9. Speleman, F., Park, J.R., and Henderson, T.O. (2016). Neuroblastoma: a tough nut to crack. Am. Soc. Clin. Oncol. Educ. Book *35*, e548–e557.
10. Mujoo, K., Cheresh, D.A., Yang, H.M., and Reisfeld, R.A. (1987). Disialoganglioside GD2 on human neuroblastoma cells: target antigen for monoclonal antibody-mediated cytolysis and suppression of tumor growth. Cancer Res. *47*, 1098–1104.
11. Smith, V., and Foster, J. (2018). High-risk neuroblastoma treatment review. Children (Basel) *5*, 114.
12. Sait, S., and Modak, S. (2017). Anti-GD2 immunotherapy for neuroblastoma. Expert Rev. Anticancer Ther. *17*, 889–904.
13. Challagundla, K.B., Wise, P.M., Neviani, P., Chava, H., Murtadha, M., Xu, T., Kennedy, R., Ivan, C., Zhang, X., Vannini, I., Fanini, F., Amadori, D., et al. (2015). Exosome-mediated transfer of microRNAs within the tumor microenvironment and neuroblastoma resistance to chemotherapy. J. Natl. Cancer Inst. *107*, djv135.
14. Neviani, P., Wise, P.M., Murtadha, M., Liu, C.W., Wu, C.H., Jong, A.Y., Seeger, R.C., and Fabbri, M. (2018). Natural Killer-derived exosomal miR-186 inhibits neuroblastoma growth and immune escape mechanisms. Cancer Res. *79*, 1151–1164.
15. Richard, H., Pokhrel, A., Chava, S., Pathania, A., Katta, S.S., and Challagundla, K.B. (2020). Exosomes: novel players of therapy resistance in neuroblastoma. Adv. Exp. Med. Biol. *1277*, 75–85.
16. Chava, S., Reynolds, C.P., Pathania, A.S., Gorantla, S., Poluektova, L.Y., Coulter, D.W., Subash, C.G., Manoj, K.P., Kishore, B.C., Gupta, S.C., Pandey, M.K., et al. (2020). miR-15a-5p, miR-15b-5p, and miR-16-5p inhibit tumor progression by directly targeting MYCN in neuroblastoma. Mol. Oncol. *14*, 180–196.

17. Gunda, V., Pathania, A.S., Chava, S., Prathipati, P., Chaturvedi, N.K., Coulter, D.W., Pandey, M.K., Durden, D.L., et al. (2020). Amino acids regulate cisplatin insensitivity in neuroblastoma. Cancers (Basel) *12*, E2576.

18. Brodeur, G.M., Seeger, R.C., Schwab, M., Varmus, H.E., and Bishop, J.M. (1984). Amplification of N-myc in untreated human neuroblastomas correlates with advanced disease stage. Science *224*, 1121–1124.

19. Puissant, A., Frumm, S.M., Alexe, G., Bassil, C.F., Qi, J., Chanthery, Y.H., Nekritz, E.A., Zeid, R., Gustafson, W.C., Greninger, P., Garnett, M.J., McDermott, U., et al. (2013). Targeting MYCN in neuroblastoma by BET bromodomain inhibition. Cancer Discov. *3*, 308–323.

20. Chan, H.S., Gallie, B.L., DeBoer, G., Haddad, G., Ikegaki, N., Dimitroulakos, J., Yeger, H., and Ling, V. (1997). MYCN protein expression as a predictor of neuroblastoma prognosis. Clin. Cancer Res. *3*, 1699–1706.

21. Huang, M., and Weiss, W.A. (2013). Neuroblastoma and MYCN. Cold Spring Harb. Perspect. Med. *3*, a014415.

22. Wenzel, A., Cziepluch, C., Hamann, U., Schürmann, J., and Schwab, M. (1991). The N-Myc oncoprotein is associated in vivo with the phosphoprotein Max(p20/22) in human neuroblastoma cells. EMBO J. *10*, 3703–3712.

23. Peifer, M., Hertwig, F., Roels, F., Dreidax, D., Gartlgruber, M., Menon, R., Krämer, A., Roncaioli, J.L., Sand, F., Heuckmann, J.M., Ikram, F., Schmidt, R., Ackermann, S., et al. (2015). Telomerase activation by genomic rearrangements in high-risk neuroblastoma. Nature *526*, 700–704.

24. Schilling, F.H., Spix, C., Berthold, F., Erttmann, R., Sander, J., Treuner, J., Michaelis, J., and Joerg, M. (2003). Children may not benefit from neuroblastoma screening at 1 year of age. Updated results of the population based controlled trial in Germany. Cancer Lett. *197*, 19–28.

25. Sawada, T., Hirayama, M., Nakata, T., Takeda, T., Takasugi, N., Mori, T., Maeda, K., Koide, R., Hanawa, Y., and Tsunoda, A. (1984). Mass screening for neuroblastoma in infants in Japan. Interim report of a mass screening study group. Lancet *2*, 271–273.

26. Woods, W.G., Tuchman, M., Robison, L.L., Bernstein, M., Leclerc, J.M., Brisson, L.C., Brossard, J., Hill, G., Shuster, J., Luepker, R., Byrne, T., et al. (1996). A population-based study of the usefulness of screening for neuroblastoma. Lancet *348*, 1682–1687.

27. Vishnoi, K., Viswakarma, N., Rana, A., and Rana, B. (2020). Transcription factors in cancer development and therapy. Cancers (Basel) *12*, 2296.

28. Darnell, J.E., Jr. (2002). Transcription factors as targets for cancer therapy. Nat. Rev. Cancer *2*, 740–749.

29. Kumar, S., Warrell, J., Li, S., McGillivray, P.D., Meyerson, W., Salichos, L., Harmanci, A., Martinez-Fundichely, A., Chan, C.W.Y., Nielsen, M.M., Lochovsky, L., et al. (2020). Passenger mutations in more than 2,500 cancer genomes: overall molecular functional impact and consequences. Cell *180*, 915–927.e6.

30. Stratton, M.R., Campbell, P.J., and Futreal, P.A. (2009). The cancer genome. Nature *458*, 719–724.

31. Bushweller, J.H. (2019). Targeting transcription factors in cancer - from undruggable to reality. Nat. Rev. Cancer *19*, 611–624.

32. Bozic, I., Antal, T., Ohtsuki, H., Carter, H., Kim, D., Chen, S., Karchin, R., Kinzler, K.W., Vogelstein, B., and Nowak, M.A. (2010). Accumulation of driver and passenger mutations during tumor progression. Proc. Natl. Acad. Sci. U S A *107*, 18545–18550.

33. Pon, J.R., and Marra, M.A. (2015). Driver and passenger mutations in cancer. Annu. Rev. Pathol. *10*, 25–50.

34. Pritchard, J., and Hickman, J.A. (1994). Why does stage 4s neuroblastoma regress spontaneously? Lancet *344*, 869–870.

35. Wu, D., Su, X., Lu, J., Li, S., Hood, B.L., Vasile, S., Potluri, N., Diao, X., Kim, Y., Khorasanizadeh, S., and Rastinejad, F. (2019). Bidirectional modulation of HIF-2 activity through chemical ligands. Nat. Chem. Biol. *15*, 367–376.

36. Capasso, M., Lasorsa, V.A., Cimmino, F., Avitabile, M., Cantalupo, S., Montella, A., De Angelis, B., Morini, M., de Torres, C., Castellano, A., Locatelli, F., et al. (2020). Transcription factors involved in tumorigenesis are over-represented in mutated active DNA-binding sites in neuroblastoma. Cancer Res. *80*, 382–393.

37. Garcia-Alonso, L., Iorio, F., Matchan, A., Fonseca, N., Jaaks, P., Peat, G., Pignatelli, M., Falcone, F., Benes, C.H., Dunham, I., Bignell, G., et al. (2018). Transcription factor activities enhance markers of drug sensitivity in cancer. Cancer Res. *78*, 769–780.

38. Su, Z., Fang, H., Hong, H., Shi, L., Zhang, W., Zhang, W., Zhang, Y., Dong, Z., Lancashire, L.J., Bessarabova, M., Yang, X., Ning, B., et al. (2014). An investigation of biomarkers derived from legacy microarray data for their utility in the RNA-seq era. Genome Biol. *15*, 523.

39. Kocak, H., Ackermann, S., Hero, B., Kahlert, Y., Oberthuer, A., Juraeva, D., Roels, F., Theissen, J., Westermann, F., Deubzer, H., Ehemann, V., et al. (2013). Hox-C9 activates the intrinsic pathway of apoptosis and is associated with spontaneous regression in neuroblastoma. Cell Death Dis. *4*, e586.

40. Henrich, K.O., Bender, S., Saadati, M., Dreidax, D., Gartlgruber, M., Shao, C., Herrmann, C., Wiesenfarth, M., Parzonka, M., Wehrmann, L., Fischer, M., et al. (2016). Integrative genome-scale analysis identifies epigenetic mechanisms of transcriptional deregulation in unfavorable neuroblastomas. Cancer Res. *76*, 5523–5537.

41. Langfelder, P., and Horvath, S. (2008). WGCNA: an R package for weighted correlation network analysis. Bioinformatics *9*, 559.

42. Herrmann, C., Van de Sande, B., Potier, D., and Aerts, S. (2012). i-cisTarget: an integrative genomics method for the prediction of regulatory features and cis-regulatory modules. Nucleic Acids Res. *40*, e114.

43. Imrichová, H., Hulselmans, G., Kalender Atak, Z., Potier, D., and Aerts, S. (2015). i-cisTarget 2015 update: generalized cis-regulatory enrichment analysis in human, mouse and fly. Nucleic Acids Res. *43*, W57–W64.

44. Aibar, S., González-Blas, C.B., Moerman, T., Huynh-Thu, V.A., Imrichova, H., Hulselmans, G., Rambow, F., Marine, J.C., Geurts, P., Aerts, J., van den Oord, J., et al. (2017). SCENIC: single-cell regulatory network inference and clustering. Nat. Methods *14*, 1083–1086.

45. Brors, B. (2010). Transcription profiling of human cells from patients with neuroblastoma in different stages, arrayexpress-repository, V1. Cell Rep. *17*, 609–623, https://www.ebi.ac.uk/arrayexpress/experiments/E-MTAB-179.

46. Ackermann, S., Cartolano, M., Hero, B., Welte, A., Kahlert, Y., Roderwieser, A., Bartenhagen, C., Walter, E., Gecht, J., Kerschke, L., Volland, R., et al. (2018). A mechanistic classification of clinical phenotypes in neuroblastoma. Science *362*, 1165–1170.

47. Cangelosi, D., Morini, M., Zanardi, N., Sementa, A.R., Muselli, M., Conte, M., Garaventa, A., Pfeffer, U., Bosco, M.C., Varesio, L., and Eva, A. (2020). Hypoxia predicts poor prognosis in neuroblastoma patients and associates with biological mechanisms involved in telomerase activation and tumor microenvironment reprogramming. Cancers (Basel) *12*, 2343.

48. Wickham, H. (2009). ggplot2. Elegant Graphics for Data Analysis (Springer), p. VIII, 213.

49. Molenaar, J.J., Koster, J., Zwijnenburg, D.A., van Sluis, P., Valentijn, L.J., van der Ploeg, I., Hamdi, M., van Nes, J., Westerman, B.A., van Arkel, J., Ebus, M.E., et al. (2012). Sequencing of neuroblastoma identifies chromothripsis and defects in neuritogenesis genes. Nature *483*, 589–593.

50. Xie, T., He, Y., Korkeamaki, H., Zhang, Y., Imhoff, R., Lohi, O., and Radhakrishnan, I. (2011). Structure of the 30-kDa Sin3-associated protein (SAP30) in complex with the mammalian Sin3A corepressor and its role in nucleic acid binding. J. Biol. Chem. *286*, 27814–27824.

51. De Bernardi, B., Carli, M., Casale, F., Corciulo, P., Cordero di Montezemolo, L., De Laurentis, C., Bagnulo, S., Brisigotti, M., Marchese, N., and Garaventa, A. (1992). Standard-dose and high-dose peptichemio and cisplatin in children with disseminated poor-risk neuroblastoma: two studies by the Italian Cooperative Group for Neuroblastoma. J. Clin. Oncol. *10*, 1870–1878.

52. Saintas, E., Abrahams, L., Ahmad, G.T., Ajakaiye, A.M., AlHumaidi, A.S., Ashmore-Harris, C., Clark, I., Dura, U.K., Fixmer, C.N., Ike-Morris, C., Mato Prado, M., et al. (2017). Acquired resistance to oxaliplatin is not directly associated with increased resistance to DNA damage in SK-N-ASrOXALI4000, a newly established oxaliplatin-resistant sub-line of the neuroblastoma cell line SK-N-AS. PLoS One *12*, e0172140.

53. Garnett, M.J., Edelman, E.J., Heidorn, S.J., Greenman, C.D., Dastur, A., Lau, K.W., Greninger, P., Thompson, I.R., Luo, X., Soares, J., Liu, Q., et al. (2012). Systematic identification of genomic markers of drug sensitivity in cancer cells. Nature *483*, 570–575.

54. Barretina, J., Caponigro, G., Stransky, N., Venkatesan, K., Margolin, A.A., Kim, S., Wilson, C.J., Lehár, J., Kryukov, G.V., Sonkin, D., et al. (2012). The Cancer Cell

Line Encyclopedia enables predictive modeling of anticancer drug sensitivity. Nature *483*, 603–607.

55. Behan, F.M., Iorio, F., Picco, G., Gonçalves, E., Beaver, C.M., Migliardi, G., Santos, R., Rao, Y., Sassi, F., Pinnelli, M., Ansari, R., et al. (2019). Prioritization of cancer therapeutic targets using CRISPR-Cas9 screens. Nature *568*, 511–516.

56. Cong, L., Ran, F.A., Cox, D., Lin, S., Barretto, R., Habib, N., Hsu, P.D., Wu, X., Jiang, W., Marraffini, L.A., and Zhang, F. (2013). Multiplex genome engineering using CRISPR/Cas systems. Science *339*, 819–823.

57. Cyranoski, D. (2016). CRISPR gene-editing tested in a person for the first time. Nature *539*, 479.

58. Yi, L., and Li, J. (2016). CRISPR-Cas9 therapeutics in cancer: promising strategies and present challenges. Biochim. Biophys. Acta *1866*, 197–207.

59. Dempster, J.M., Pacini, C., Pantel, S., Behan, F.M., Green, T., Krill-Burger, J., Beaver, C.M., Younger, S.T., Zhivich, V., Najgebauer, H., Allen, F., et al. (2019). Agreement between two large pan-cancer CRISPR-Cas9 gene dependency data sets. Nat. Commun. *10*, 5817.

60. Doench, J.G., Fusi, N., Sullender, M., Hegde, M., Vaimberg, E.W., Donovan, K.F., Smith, I., Tothova, Z., Wilen, C., Orchard, R., Virgin, H.W., et al. (2016). Optimized sgRNA design to maximize activity and minimize off-target effects of CRISPR-Cas9. Nat. Biotechnol. *34*, 184–191.

61. Ruiz-Pérez, M.V., Henley, A.B., and Arsenian-Henriksson, M. (2017). The MYCN protein in health and disease. Genes (Basel) *8*, 113.

62. Zimmerman, K.A., Yancopoulos, G.D., Collum, R.G., Smith, R.K., Kohl, N.E., Denis, K.A., Nau, M.M., Witte, O.N., Toran-Allerand, D., and Gee, C.E. (1986). Differential expression of myc family genes during murine development. Nature *319*, 780–783.

63. Stanton, B.R., Perkins, A.S., Tessarollo, L., Sassoon, D.A., and Parada, L.F. (1992). Loss of N-myc function results in embryonic lethality and failure of the epithelial component of the embryo to develop. Genes Dev. *6*, 2235–2247.

64. Knoepfler, P.S., Cheng, P.F., and Eisenman, R.N. (2002). N-myc is essential during neurogenesis for the rapid expansion of progenitor cell populations and the inhibition of neuronal differentiation. Genes Dev. *16*, 2699–2712.

65. Nagy, A., Moens, C., Ivanyi, E., Pawling, J., Gertsenstein, M., Hadjantonakis, A.K., Pirity, M., and Rossant, J. (1998). Dissecting the role of N-myc in development using a single targeting vector to generate a series of alleles. Curr. Biol. *8*, 661–664.

66. Rickman, D.S., Schulte, J.H., and Eilers, M. (2018). The expanding world of N-MYC-Driven tumors. Cancer Discov. *8*, 150–163.

67. Zimmerman, M.W., Liu, Y., He, S., Durbin, A.D., Abraham, B.J., Easton, J., Shao, Y., Xu, B., Zhu, S., Zhang, X., Li, Z., et al. (2018). MYC drives a subset of high-risk pediatric neuroblastomas and is activated through mechanisms including enhancer hijacking and focal enhancer amplification. Cancer Discov. *8*, 320–335.

68. Westermann, F., Muth, D., Benner, A., Bauer, T., Henrich, K.O., Oberthuer, A., Brors, B., Beissbarth, T., Vandesompele, J., Pattyn, F., Hero, B., et al. (2008). Distinct transcriptional MYCN/c-MYC activities are associated with spontaneous regression or malignant progression in neuroblastomas. Genome Biol. *9*, R150.

69. Hadjidaniel, M.D., Muthugounder, S., Hung, L.T., Sheard, M.A., Shirinbak, S., Chan, R.Y., Nakata, R., Borriello, L., Malvar, J., Kennedy, R.J., Iwakura, H., et al. (2017). Tumor-associated macrophages promote neuroblastoma via STAT3 phosphorylation and up-regulation of c-MYC. Oncotarget *8*, 91516–91529.

70. Berthold, F., Rosswog, C., Christiansen, H., Frühwald, M., Hemstedt, N., Klingebiel, T., Fröhlich, B., Schilling, F.H., Schmid, I., Simon, T., et al. (2021). Clinical and molecular characterization of patients with stage 4(M) neuroblastoma aged less than 18 months without MYCN amplification. Pediatr. Blood Cancer *68*, e29038.

71. Moroz, V., Machin, D., Faldum, A., Hero, B., Iehara, T., Mosseri, V., Ladenstein, R., De Bernardi, B., Rubie, H., Berthold, F., Matthay, K.K., et al. (2011). Changes over three decades in outcome and the prognostic influence of age-at-diagnosis in young patients with neuroblastoma: a report from the International Neuroblastoma Risk Group Project. Eur. J. Cancer *47*, 561–571.

72. Haupt, R., Garaventa, A., Gambini, C., Parodi, S., Cangemi, G., Casale, F., Viscardi, E., Bianchi, M., Prete, A., Jenkner, A., Luksch, R., et al. (2010). Improved survival of children with neuroblastoma between 1979 and 2005: a report of the Italian Neuroblastoma Registry. J Clin Oncol *28*, 2331–2338.

73. Formicola, D., Petrosino, G., Lasorsa, V.A., Pignataro, P., Cimmino, F., Vetrella, S., Longo, L., Tonini, G.P., Oberthuer, A., Iolascon, A., Fischer, M., et al. (2016). An 18 gene expression-based score classifier predicts the clinical outcome in stage 4 neuroblastoma. J. Transl Med. *14*, 142.

74. Ham, J., Costa, C., Sano, R., Lochmann, T.L., Sennott, E.M., Patel, N.U., Dastur, A., Gomez-Caraballo, M., Krytska, K., Hata, A.N., Floros, K.V., et al. (2016). Exploitation of the apoptosis-primed state of MYCN-amplified neuroblastoma to develop a potent and specific targeted therapy combination. Cancer Cell *29*, 159–172.

75. Blume-Jensen, P., and Hunter, T. (2001). Oncogenic kinase signalling. Nature *411*, 355–365.

76. Gross, S., Rahal, R., Stransky, N., Lengauer, C., and Hoeflich, K.P. (2015). Targeting cancer with kinase inhibitors. J. Clin. Invest. *125*, 1780–1789.

77. Stransky, N., Cerami, E., Schalm, S., Kim, J.L., and Lengauer, C. (2014). The landscape of kinase fusions in cancer. Nat. Commun. *5*, 4846.

78. Russo, R., Cimmino, F., Pezone, L., Manna, F., Avitabile, M., Langella, C., Koster, J., Casale, F., Raia, M., Viola, G., Fischer, M., Iolascon, A., et al. (2017). Kinome expression profiling of human neuroblastoma tumors identifies potential drug targets for ultra high-risk patients. Carcinogenesis *38*, 1011–1020.

79. Jemaà, M., Sime, W., Abassi, Y., Lasorsa, V.A., Bonne Køhler, J., Michaelis, M., Cinatl, J., Capasso, M., and Massoumi, R. (2020). Gene expression signature of acquired chemoresistance in neuroblastoma cells. Int. J. Mol. Sci. *21*, 6811.

80. Brodeur, G.M., Pritchard, J., Berthold, F., Carlsen, N.L., Castel, V., Castelberry, R.P., De Bernardi, B., Evans, A.E., Favrot, M., and Hedborg, F. (1993). Revisions of the international criteria for neuroblastoma diagnosis, staging, and response to treatment. J. Clin. Oncol. *11*, 1466–1477.

81. Cohen, M.D. (1994). International criteria for neuroblastoma diagnosis, staging, and response to treatment. J. Clin. Oncol. *12*, 1991–1993.

82. Challagundla, K.B., Sun, X.X., Zhang, X., DeVine, T., Zhang, Q., Sears, R.C., and Dai, M.S. (2011). Ribosomal protein L11 recruits miR-24/miRISC to repress c-Myc expression in response to ribosomal stress. Mol. Cell. Biol. *31*, 4007–4021.

83. Yang, W., Soares, J., Greninger, P., Edelman, E.J., Lightfoot, H., Forbes, S., Bindal, N., Beare, D., Smith, J.A., Thompson, I.R., Ramaswamy, S., et al. (2013). Genomics of Drug Sensitivity in Cancer (GDSC): a resource for therapeutic biomarker discovery in cancer cells. Nucleic Acids Res. *41*, D955–D961.